Shift of annual water balance in the Budyko space for catchments with groundwater dependent evapotranspiration

X.-S. Wang[1] and Y. Zhou[2]

[1]{Ministry of Education Key Laboratory of Groundwater Circulation and Evolution, China University of Geosciences, Beijing 100083, China }

[2]{UNESCO-IHE Institute for Water Education, Delft, The Netherlands }

Correspondence to: X.-S. Wang (wxsh@cugb.edu.cn)

Abstract

The Budyko framework represents the general relationship between the evapotranspiration ratio (F) and the aridity index (ϕ) for the mean annual water balance at catchment scale. It is interesting to investigate if this standard F-ϕ space can be also applied to capture the shift of annual water balance in catchments with the varying dryness. There are reported cases where the original Budyko framework can not be directly applied for annual water balance due to additional sources of water supply for evapotranspiration besides precipitation. This study investigates how groundwater dependent evapotranspiration causes the shift of annual water balance in the standard Budyko space. A widely used monthly hydrological model, the ABCD model, is modified to incorporate groundwater dependent evapotranspiration in the zone with shallow water table and delayed groundwater recharge in the zone with deep water table. This model is applied in six catchments in the Erdos Plateau, China, to estimate the actual annul evapotranspiration. Results show that the variations in the annual F value with the aridity index do not satisfy the normal Budyko formulas. The shift of the annual water balance in the standard Budyko space is a combination of the Budyko-type response in the deep groundwater zone and the quasi-energy limited condition in the shallow groundwater zone. Excess evapotranspiration (F>1) could occur in dry years, which is contributed by the

significant supply of groundwater for evapotranspiration. Use of groundwater for irrigation can increase the frequency of the $F>1$ cases.

1 Introduction

Estimating catchment water balance is one of the fundamental tasks in hydrology. Efforts have long been devoted to construct the physical, empirical, and statistical models to explain the general relationship among precipitation (P), runoff (Q), potential evapotranspiration (E_0) and actual evapotranspiration (E) in terms of mean annual fluxes at the catchment scale (Budyko, 1948, 1958, 1974; Mezentsev, 1955; Fu, 1981; Porporato et al., 2004; Gerrits et al., 2009). A simple and highly intuitive approach widely used for estimating E at mean annual water balance is the Budyko framework, in which the mean annual evapotranspiration ratio (E/P) was presumed as a function of the climatic dryness as:

$$\frac{E}{P} = F\left(\frac{E_0}{P}\right) = F(\phi) \quad (1)$$

where ϕ is the aridity index defined as E_0/P, and $F(\phi)$ is an empirical function that relates E/P to ϕ based on general water-energy balance. The proposed formula by Budyko (1958; 1974) was:

$$F(\phi) = \sqrt{\phi[1-\exp(-\phi)]\tanh(1/\phi)} \quad (2)$$

which indicates a nonlinear relation between F and ϕ. This F-ϕ curve has been called the Budyko curve (Zhang et al., 2004; Roderick and Farquhar, 2011) and the F-ϕ space was called Budyko space (Renner et al., 2012).

Instead of using a single curve determined by Eq. (2) in the Budyko space, researchers have introduced a specific catchment parameter in $F(\phi)$ to consider the impacts of catchment properties such as soils and vegetation (Mezentsev, 1955; Fu, 1981; Zhang et al., 2001). For example, Fu's equation (Fu, 1981) was derived following the idea of Mezentsev (1955), which can be expressed as follows:

$$F(\phi, w) = 1+\phi-(1+\phi^w)^{1/w} \quad (3)$$

where w is a parameter represents the catchment conditions. F increases with w, leading to reduced Q/P as w grows (Fu, 1981). Fu's equation has been widely used in the last decade (Zhang et al., 2004; Yang et al., 2006; Yang et al., 2007; Zhang et al., 2008; Greve et al., 2015). Donohue (2007) highlighted the role of vegetation dynamics in the application of the Budyko framework. Recently, Wang and Tang (2014) also developed a one-parameter Budyko model based on the proportionality hypothesis and revealed a complex relationship between the catchment specific parameter (w in Eq. (3)) and the remote sensing vegetation index. These modified formulas suggested a group of Budyko curves instead of the single original Budyko curve, in which a curve represents a specific type of the catchments with similar features controlling the mean annual water balance.

Budyko hypothesis has been directly used to analyze the interannual change in water balance in catchments (Arora, 2002; Zhang et al., 2008; Potter and Zhang, 2009) even through ignoring the change in storage (ΔS) under the assumption of steady state water balance. One can plot annually the estimated E/P data in the standard Budyko space to check whether the normal Budyko curves are sufficient or not to represent the interannual variability of evapotranspiration with the varying dryness. In this way, Potter and Zhang (2009) found that the Budyko framework is generally applicable for the catchments in Australia and the optimal curve of annual E/P versus ϕ is highly dependent on the seasonal variations in rainfall. However, this approach should be carefully used when the E/P values are approximated by $(P-Q)/P$ values. Wang et al. (2009) and Istanbulluoglu et al. (2012) reported that the annual data of $(P-Q)/P$ in some basins are negatively related to the aridity index, exhibiting an inverse trend in comparison with the normal Budyko curves. According to long-term groundwater observations in the North Loup River basin, Nebraska, USA, Istanbulluoglu et al. (2012) demonstrated that the annual E/P values estimated by $(P-Q-\Delta G)/P$ basically follows the Budyko hypothesis, where ΔG is the change in groundwater storage. However, in some other studies, an unexpected high evapotranspiration ratio ($E/P>1$) was observed (Cheng et al., 2011; Wang, 2012; Chen et al., 2013). Among the 12 watersheds investigated by Wang (2012), half of them exhibited such high E/P values in two or more drought years. The physical base of the phenomena is the significant contribution of storage in extremely arid situations by which the high level of evapotranspiration is maintained. Although some of the cases due to extracting groundwater for irrigation in farmlands (Cheng et al., 2011; Wang, 2012), it could occur in natural conditions as a result of the temporal redistribution of water

from seasonal patterns (Chen et al., 2013). Wang (2012) and Chen et al. (2013) proposed an approach to extend the Budyko framework for annual or even intra-annual water balance by considering the soil water storage as a potential source of water supply for evapotranspiration. They define $P-\Delta S$ for the selected time scales as the effective rainfall in building the modified Budyko space with $E/(P-\Delta S)$ and $E_0/(P-\Delta S)$, instead of E/P and ϕ, respectively.

The excess annual evapotranspiration may be originated from both soil water and groundwater. As reported by Wang (2012), during the drought year in 1988, two watersheds in Illinois, USA, showed E/P=1.1 with ~100 mm depletion in soil water and ~200 mm decrease in groundwater storage, respectively. It seemed that the contribution of groundwater is more significant (partially enhanced by pumping). Small depth to water table is an advantage to keep a high level of soil water content near ground surface for evapotranspiration (Chen and Hu, 2004). Therefore, it could be argued that the existence of shallow groundwater in a catchment would enhance the occurrence of $E/P>1$ in drought years. Groundwater dependent evapotranspiration at the regional scale has been noticed in the previous studies (York et al, 2002; Chen and Hu, 2004; Cohen et al., 2006; Yeh and Famiglietti, 2009). Nevertheless, little has been known on the role of groundwater in the interannual variability of the evapotranspiration ratio with the varying dryness. Chen et al. (2013) did not identify the change in groundwater storage to explain the controls of the $E/P>1$ cases. Wang (2012) mentioned the potential role of groundwater in occurrence of the $E/P>1$ cases but the individual contribution of groundwater dependent evapotranspiration was not soundly analyzed.

This study aims to investigate how groundwater dependent evapotranspiration influences the annual water balance behavior in the standard Budyko space and develop a modified formula to consider this effect. A monthly hydrological model was developed from the widely used ABCD model (Thomas, 1981) to incorporate the groundwater dependent evapotranspiration as well as the deep infiltration in the vadose zone. The value of E was partitioned into two components in accounting for the individual roles of the normal soil water dependent and the specific groundwater dependent evapotranspiration. Then, the modified model was applied to 6 catchments in the Erdos Plateau, China. The calibrated model was used to produce the annual time series of the evapotranspiration components linking with the variable soil water storage and groundwater storage. With varying climatic dryness, the shift behaviors of the interannual water balance in the standard and modified Budyko space for the catchment were

analyzed in detail. The impacts of human activities were also discussed. The study reveals the contribution of groundwater in the interannual variability of catchment water balance under a changing climate.

2 Study Area, Data and Preliminary Analysis

2.1 River Basins

The study area is located in the Erdos Plateau in north-central China (Fig. 1a), belongs to the middle part of the Yellow River Basin. The climate of the Erdos Plateau is typically inland semiarid to arid with a significant gradient of the mean annual precipitation, from 150 mm in the west to 450 mm in the east (Fig. 1b). More than half of the annual precipitation is received in the warm season (from June to September). Six catchments with available data, numbered as C1-C6 (Fig. 1b), are selected for this study. The areas of the catchments range between 1,272 km^2 and 3,253 km^2.

In particular, C1 is the Hailiutu River catchment (HRC), with an area of 2,645 km^2, which lies on the southeast edge of the Mu Us Desert and is a sub-catchment of the Wuding River basin (Fig. 1b). The main channel of the HRC has a length of approximately 85 km and flows southwards to the Hanjiamao hydrological station, as shown in Fig. 1c. Due to the arid climate and desert landscape, the land cover within the catchment is characterized by desert sand dunes with patches of mostly shrublands. Depression areas and terrace lands with shallow groundwater are covered by meadows and some farmlands. Wind-breaking trees (*Salix matsudana* and *Populus tomentosa*) can be found along the roads and crop areas. Farmlands are mainly located in the southern area and especially in the river valley. Crops cover only ~3% of the total catchment area. Maize is the dominant crop and is irrigated with streamflow and/or groundwater. Several diversion dams have been constructed along the Hailiutu River since the early 1970s for irrigation.

The other catchments have different characteristics. C2 is also located in the Wuding River basin but mainly covered by loess sediments and shows a more undulating landscape than that in the HRC. The landscape of C3 is a mixture of the desert sand dunes in the west and the loess hills in the east. C4-C6 are mainly located in the loess hills region with steep slopes and deep valleys. Among them, C4 is the upstream area of a larger river basin with more flat

landscape than the downstream topography. A lot of ravines exist in the loess hills region by which floods can be released to the rivers. Soil and water conservation projects have been conducted to control the floods and sediment loss. A comparison of the hydrological behaviors between C1 and C6 has been presented by Zhou et al. (2015).

In the study area, groundwater is stored in complex aquifer systems. In general, the Erdos Plateau is characterized by shallow groundwater in the sandy sediments and deep groundwater in the underlying sandstones. In C1-C2, the Cretaceous sandstones form a thick aquifer enabling active groundwater circulation. In C3~C6, the Cretaceous sandstones is limited or replaced by the Jurassic sandstone-mudstone formations with lower permeability so that the movement of deep groundwater is restricted. Meanwhile, shallow groundwater exists in the valleys or near-lake areas covered by sandy or loess sediments. Regional groundwater level distribution in the HRC has been investigated in Lv et al. (2013) based on a hydrogeological survey carried out in 2010. According to this investigation, depth to water table (DWT) in the HRC varies in a large range from zero to 110 m. In more than half of the area, DWT is less than 10 m. The shallow groundwater zone, where DWT is no more than 2 m, occupies 16.0% of the whole catchment area. As investigated in Yin et al. (2015) at the site of the HRC, when DWT is less than 2 m, the evapotranspiration would be generally 80% or more of the potential, whereas the evapotranspiration ratio is generally less than 0.4 for the deep groundwater condition. This investigation confirms that groundwater dependent evapotranspiration is an essential process in the Erdos Plateau.

2.2 Data

Daily streamflow data since 1957 for the hydrological stations at the outlets of the 6 catchments were collected from the Yellow River Conservancy Commission. A rainfall gauge was also installed at the Hanjiamao hydrological station (Fig. 1c) in 1961, providing daily precipitation.

To better account for the variability of rainfall in space and time, we developed gridded monthly precipitation data with 1-km resolution between 1957 and 2010 from the data of 15 national meteorological stations in the Erdos Plateau (Fig. 1b). Monthly rainfall data at these stations were downloaded from the China Meteorological Data Sharing Service System (CMDSSS, http://cdc.nmic.cn). We constructed the gridded data using the inverse distance square weighting (IDSW) method due to the moderate topography of the Erdos Plateau in the

form of low-relief rolling hills. Fig. 1b shows the mean annual precipitation contours of the Erdos Plateau obtained from the gridded data. In this study, the area-averaged monthly precipitation in the 6 catchments for the period 1957-2010 was estimated by imposing the basins boundaries on the gridded monthly precipitation data and taking the arithmetic average of the cell values within the catchment.

The method applied in constructing the gridded precipitation data were further applied in constructing a 1-km resolution gridded dataset for the monthly pan evaporation between 1957 and 2010 covering the Erdos Plateau. The pan evaporation data were based on observations from 200-mm diameter pans that were installed in most stations in the Erdos Plateau and can be also downloaded from CMDSSS (http://cdc.nmic.cn). The average monthly potential evapotranspiration (E_0) in the 6 catchments was estimated from the spatially averaged data of pan evaporation using a local pan coefficient (0.58) for the 200-mm diameter pan. This coefficient was suggested by various investigations of pan coefficients for Chinese meteorological stations (Shi et al., 1986; Fan et al., 2006).

In summary, the mean annual values of P, E_0 and Q during the period in 1957-1978 for the 6 catchments are listed in Table 1. In this period, the streamflow is not significantly influenced by the hydraulic engineering, irrigation water use and coal mine industry so that the hydrological behavior is close to the natural state. It can be estimated from the data that the mean annual Q/P values in this 'natural' state ranged between 0.1 and 0.3 for the 6 catchments. Accordingly, the mean annual E/P values are higher than 0.7 with respect to the mean values of the aridity index (E_0/P) varying between 2.5 and 3.4.

In Fig. 2a, the variation patterns of the monthly rainfall and potential evapotranspiration during 1957-2010 are shown for the HRC. Both rainfall and evapotranspiration are high in the summer and low in the winter. However, there is a difference in the patterns by which the seasonal variation in runoff may be influenced: the rainfall peak normally arrives in the August but the highest evaporation is exhibited in the June. With respect to these meteorological patterns, the total runoff drops in the Spring and in the early Summer until the heavy rainfall comes in the August, as shown in Fig. 2b. In comparison with the rainfall and the potential evapotranspiration, the mean monthly runoff (2.6 mm) and its fluctuation amplitude (0.8-11.9 mm) are quite small. This indicates that most of the precipitation in the HRC returns to the atmosphere by evapotranspiration. During 1957 to 2010, the annual aridity

index in the HRC showed a large variation range (between 1 and 10), covering the semi-humid, semi-arid and arid climatic conditions as classified in the scheme recommended by the United Nations Environment Programme (UNEP) (Middleton and Thomas, 1992).

In the study area, there are significant interannual fluctuations in streamflow. For the HRC, Yang et al. (2012) investigated the annual regime shifts in streamflow and found that the shifts was caused largely by land use policy changes and river water diversions for irrigation. Tab. 2 shows the mean annual fluxes in four typical periods with different numbers of diversions in the Hailiutu River and major branches during 1957-2010. These diversions influenced the hydrological behavior in the HRC and will be discussed in the following sections. However, before 1967, the Hailiutu River was free of hydraulic engineering, and the studied area was mostly close to the natural conditions. In the other catchments, the changes in the streamflow regime were also mainly contributed by human activities but in more complex ways. In C6, the river discharge was also influenced by a large number of check dams that constructed to reduce water and sediment loss (Zhou et al., 2015). In C3-C5, the impacts of coal mining industry were significant. To analyze the natural hydrological behaviors, the study period should not be later than 1978.

2.3 Preliminary analysis using $(P–Q)/P$

In many cases, it is possible to estimate the annual E in a catchment from the annually observed P and Q by $P–Q$ when the change in storage is sufficiently small. Then it could be treated as the "real" data of the annual E and the shift of annual water balance in the Budyko space could be investigated with the plot of $(P–Q)/P$ versus E_0/P. In this section, we check the validity of this approach in the study area.

The plots of annual $(P–Q)/P$ versus E_0/P during 1957-1878 (close to natural state) for the 6 catchments are shown in Fig. 3. In particular, Fig. 3a shows the locations of the mean annual $(P–Q)/P$ data of the 6 catchments in the Budyko space. The data points fall below the original Budyko curve given by Eq. (2) but can be bounded between two modified Budyko curves that determined using Eq. (3). They approximately exhibit a normal positive trend in $(P–Q)/P$ versus E_0/P. It indicates that the behaviors of the catchments in long-term average (22-years) satisfied the steady state water balance assumption in the original Budyko framework.

If the original Budyko formula (Budyko, 1958) is available for the annual water balance, the annual $(P–Q)/P$ value should be equal to $F(\phi)$ so that the shift path of $(P–Q)/P$ in each catchment should be an increasing curve with a positive slope in the Budyko space. However, as shown in Fig. 3(b-d), the annual $(P–Q)/P$ data in C1-C4 follow negative trends. The annual $(P–Q)/P$ value of C3 significantly decreased from ~0.8 to ~0.5 when the aridity index increased from 1.2 to 5.8 (Fig. 3c). It seems that C5 (Fig. 3e) and C6 (Fig. 3f) showed normal trends but the data points did not fall well along the original Budyko curve. The negative trends in C1-C4 are contrary to the positive E/P trend in the original Budyko framework, indicating the false of taking the annual $(P–Q)/P$ as the replica of the annual E/P in the study area. In a previous study, Istanbulluoglu et al. (2012) also highlighted this abnormal trend in the North Loup River basin, Nebraska, USA, and they demonstrated that the trend was due to ignoring the change in storage. They used long-term monitoring data of groundwater level to estimate the inter-annual change in groundwater storage (ΔG) and replaced the $(P–Q)/P$ data with the $(P–Q–\Delta G)/P$ data to reproduce a normal Budyko curve for the basin.

It is a good idea to estimate the change in groundwater storage using groundwater monitoring data. However, long-term groundwater level monitoring data were not available for the catchments in this study. In addition, the approach of using $(P–Q–\Delta G)/P$ data still has a risk in ignoring the inter-annual change in the soil moisture storage. In this investigation, we used a hydrological model to estimate the actual annual E from the monthly steps, in which the groundwater dependent evapotranspiration is incorporated. With the model, both the storage components and the contribution of groundwater for the annual E can be obtained at the catchment scale.

3 Hydroclimatologic models

3.1 The ABCD model

The ABCD model is a conceptual hydrological model with 4 parameters (a, b, c, and d) developed by Thomas (1981) to account for the actual evapotranspiration, surface/sub-surface runoff and storage changes. The ABCD model was originally applied at an annual time step but has been recommended as a monthly hydrological model (Alley, 1984). It was widely applied as a hydroclimatologic model to investigate the response of catchments to climate

change (Vandewiele et al., 1992; Fernandez et al., 2000; Sankarasubramanian and Vogel, 2002; Li and Sankarasubramanian, 2012).

Both the soil water and groundwater are considered in the ABCD model, as shown in Fig. 4a. At the monthly time step, the change in the soil water storage is determined by:

$$W_m - W_{m-1} = P_m - E_m - R_m \quad (4)$$

where W_{m-1} and W_m are the effective soil water storages at the beginning and at the end of the m-th month, respectively; P_m and E_m are the monthly precipitation and evapotranspiration values, respectively; and R_m is the monthly loss of soil water via direct runoff and groundwater recharge. The change in groundwater storage is determined by:

$$G_m - G_{m-1} = cR_m - dG_m \quad (5)$$

where G_{m-1} and G_m represent the groundwater storage at the beginning and the end of the m-th month, respectively; c and d are two parameters that account for groundwater recharge and discharge from R_m and G_m, respectively. The monthly streamflow is the summation of the monthly direct runoff and groundwater discharge, as follows:

$$Q_m = (1-c)R_m + dG_m \quad (6)$$

The change in storage in the ABCD model is the summation of the changes in the soil water storage and groundwater storage, which can be expressed as $(W_m - W_{m-1}) + (G_m - G_{m-1})$.

Thomas (1981) proposed a nonlinear function to estimate $(E_m + W_m)$ from $(P_m + W_{m-1})$ as follows:

$$E_m + W_m = \frac{P_m + W_{m-1} + b}{2a} - \sqrt{\left(\frac{P_m + W_{m-1} + b}{2a}\right)^2 - \frac{(P_m + W_{m-1})b}{a}} \quad (7)$$

where a is a dimensionless parameter, and b is the upper limit of $(E_m + W_m)$. In addition, Thomas (1981) assumed:

$$W_m = (E_m + W_m)\exp(-E_{0m}/b) \quad (8)$$

where E_{0m} is the monthly potential evaporation for the m-th month. Substituting Eq. (8) into Eq. (7), the monthly evapotranspiration can be estimated as:

$$E_m = \left[\frac{P_m + W_{m-1} + b}{2a} - \sqrt{\left(\frac{P_m + W_{m-1} + b}{2a}\right)^2 - \frac{(P_m + W_{m-1})b}{a}}\right]\left[1 - \exp\left(-\frac{E_{0m}}{b}\right)\right] \quad (9)$$

Wang and Tang (2014) demonstrated that Eq. (7) can be derived from the generalized proportionality principle and yield an equivalent Budyko-type model.

3.2 The ABCD-GE model

To investigate the effects of groundwater dependent runoff and evapotranspiration in basins with both shallow and deep groundwater, the original ABCD model is extended in this study as the ABCD-GE model where 'GE' denotes groundwater dependent evapotranspiration. As shown in Fig. 4b, a catchment is conceptually divided into two zones where the Zone-1 and Zone-2 represent different areas with deep and shallow groundwater, respectively. Direct runoff is originated from both zones. Surface water (water in river, canals, lakes, etc.) is also included in the Zone-2. The soil water reservoir in the Zone-1 is the same as that in the ABCD model. In addition, a transition vadose zone is specified between the soil layer and water table to represent the delayed groundwater recharge. The transition zone is included to handle the existence of thick unsaturated zone (>10 m) in a basin. Soil water in this zone is dominated by vertical downward flow. In the Zone-2, rainfall and evapotranspiration are the components directly involved in the water balance of groundwater. Thus, three storage components are considered as a chain in the hydrological processes. It is assumed that the potential change in groundwater storage by the lateral flow coming in and out of a catchment could be ignored. For a large river basin (>1000 km^2) this assumption is generally acceptable.

Dividing the Zone-1 and Zone-2 in a catchment depends on how groundwater can be accessed by evapotranspiration. It is controlled by the depth of plant roots and the rise of capillary water above water table. In the case study of the HRC, it was observed that some trees have long roots penetrated 2-3 m or more into the earth (Lv et al., 2013), but in general the dominant root zone is less than 2 m below ground surface for shrubs and grasses. When the DWT is larger than 2 m, the contribution of groundwater for evapotranspiration will dramatically decrease to a negligible level (Yin et al., 2015). Thus, it is reasonable to use the contours of 2-m-depth of groundwater as the approximate boundary of the Zone-1 and Zone-2 in the study area. In the Zone-1, the transition vadose zone is roughly defined as the zone between 2-m-depth below ground surface and 2-m-height above water table. In the

assumptions of the ABCD-GE model, this zone could not be influenced by both the evapotranspiration and groundwater flow processes. Thus, the thickness of the soil layer would be less than 2 m in the model. However, one should be aware of that it is not necessary to find the distinct and exact boundaries for the zones, since the ABCD-GE model is a conceptual hydrological model.

Similar to that in the ABCD model, the change in the soil water storage in the Zone-1 is determined by:

$$W_m - W_{m-1} = P_m - E_{1m} - R_m \quad (10)$$

where $E_{1\mathrm{m}}$ is the monthly evapotranspiration in the Zone-1 determined with Eq. (9); R_m becomes the summation of the leaking soil water to the transition vadose zone, cR_m, and the direct runoff, $(1-c)R_m$, in the Zone-1. The change in storage of the vadose zone is described with:

$$V_m - V_{m-1} = cR_m - kV_m \quad (11)$$

where V_m and V_{m-1} represent the values of storage in the transition vadose zone at the end and beginning of the m-th month, respectively; c is the constant similar to that used in the ABCD model; and k is the parameter that accounts for groundwater recharge rate as kV_m.

In the ABCD-GE model, the source of direct runoff is partitioned by the fractions of the area of the two zones. The total runoff in the catchment is the summation of the direct runoff and groundwater discharge as follows:

$$Q_m = (1-\alpha)(1-c)R_m + \alpha(1-c)P_m + dG_m \quad (12)$$

where α is the ratio of the Zone-2 area to the whole catchment area. In Eq. (12), the term $(1-\alpha)(1-c)R_m$ denotes the direct runoff contributed by the Zone-1 and $\alpha(1-c)P_m$ denotes the direct runoff contributed by the Zone-2. In considering of the gain-loss processes of groundwater, the change in the effective groundwater storage is yielded by:

$$G_m - G_{m-1} = (1-\alpha)kV_m + \alpha(cP_m - E_{2m}) - dG_m \quad (13)$$

where $E_{2\mathrm{m}}$ is the monthly evapotranspiration in the Zone-2, which depends on the effective groundwater storage as follows:

$$E_{2m} = gG_m E_{0m} \qquad (14)$$

where g is a parameter controlling the intensity of groundwater dependent evapotranspiration. Eq. (14) assumes that the evapotranspiration rate in the Zone-2 is simply proportional to both the groundwater storage (which is positively related to groundwater level) and the potential evapotranspiration rate. Thus, the evapotranspiration rate as a whole in the catchment is summarized as

$$E_m = (1-\alpha)E_{1m} + \alpha E_{2m} \qquad (15)$$

Eqs. (10)-(13) are solved one by one and finally the value of G_m is substituting into Eq. (12) to obtain the runoff. The solutions of the ABCD-GE model are controlled by 7 parameters as: a, b, c, d, g, k and α. The parameter values should be identified with the model calibration process.

4 Model Calibration and Results

4.1 Model calibration

We applied the ABCD-GE model to estimate the monthly evapotranspiration and the change in storage in the catchments after the model parameters were calibrated. The monthly evapotranspiration data were then summed up to estimate the annual evapotranspiration for further analysis. The model calibration was based on the observed monthly streamflow data at the hydrological stations and the separated baseflow data.

Because groundwater discharge has been included in the model, a baseflow analysis was performed to obtain the expected groundwater discharge for the model calibration. Using the automated hydrograph separation method HYSEP (Sloto and Crouse, 1996) on the daily streamflow data, such 'observed' groundwater discharge data were obtained. For the HRC, these data were partly reported in Zhou et al. (2013). The mean values of the baseflow index for C1-C6 range between 0.13 and 0.88 (Table 1). The HRC has the highest baseflow index (0.88), indicating that groundwater discharge is the dominant hydrological process in this catchment. Variation patterns of the monthly groundwater discharge in the HRC are shown in

Fig. 2b. In C5 and C6, the baseflow index values are smaller than 0.2 because most of the streamflow is contributed by direct runoff.

The ordinary least squares (OLS) criterion was applied for parameter estimation. The errors of both log-streamflow and log-baseflow were included in the OLS objective function, as follows:

$$\min U = \sum_{m=1}^{N} \left(e_m^2 + q_m^2 \right) \qquad (16)$$

Where:

$$e_m = \ln(\hat{Q} / Q)_m, \quad q_m = \ln(\hat{Q}_b / Q_b)_m \qquad (17)$$

and U is the value of the objective function; N is the number of months; $\hat{Q}$ and Q are the simulated and observed monthly streamflow, respectively; $\hat{Q}_b$ is the simulated monthly groundwater discharge through dG_m in Eq. (12); and Q_b is the 'observed' monthly groundwater discharge obtained from the baseflow analysis. The log form errors given in Eq. (17) can be used to obtain homoscedastic residuals (rather than the residual errors) of the normal absolute differences between the observed data and the model outputs (Alley, 1984). The nonlinear optimization algorithm Generalized Reduced Gradient (GRG) (Lasdonet al., 1978) was used to determine the optimum values of the parameters. The Nash-Sutcliffe efficiency (NSE) (Nash and Sutcliffe, 1970) was also applied to evaluate the performance of the model in simulating the monthly runoff. It ranges in (–∞, 1) whereas a higher than zero value is required for a well-perform model.

For the HRC, the model parameters were firstly identified using the 1957-1966 data, and this calibrated model was considered to be a 'natural' model due to the minimum impact of human activities during this 10-years period. For C2-C6, the 1957-1978 period is applied to roughly identify the 'natural' model according to the general shift patterns of the annual streamflow. The initial storage values were also regarded as the unknown parameters to be determined in the calibration process. Changes in the initial conditions generally influenced the simulated results in the first and second years. Therefore, the residual errors in the later years were applied to estimate the parameter values with less influence from the initial

conditions. A sensitivity analysis was carried out to schematically capture the ranges of the parameter values.

The best fitting parameter values of the 'natural' model for C1-C6 are shown in Table 3. The *a* value ranges between 0.91 and 0.97. In previous studies using the ABCD model, the *a* value was found generally to be higher than 0.9 (Alley, 1984; Sankarasubramanian and Vogel, 2002; Li and Sankarasubramanian, 2012). The *b* and *c* values are generally higher than that obtained by Alley (1984) for ten catchments in the USA. The higher *c* value indicates more significant role of groundwater in the hydrological behaviors. However, the *d* values of C1-C6 fall into the range suggested by Alley (1984). The optimized α value in the 'natural' model ranges between 0.09 and 0.27 for different catchments. In particular, the α value of the HRC (0.21) in this 'natural' state was larger than the current value (DWT in 16.0% of the area is less than 2 m). Such a difference is reasonable because groundwater level in the 1950s and 1960s should be higher than that at present as indicated by the higher baseflow (Fig. 2b). The *k* value controls the rate of groundwater recharge below the transition vadose zone. The transition vadose zone is a necessary component in C1-C3 as demonstrated by the sensitivity analysis. When an extremely high value of *k* is used (k >100), the kV_m value would be almost equal to cR_m so that the transition vadose zone does not make sense. However, in this situation the model could never capture the seasonal variation patterns of groundwater discharge. Thus, the delayed groundwater recharge is an essential process for the catchments. The best fitting *k* values for C4-C6 are significantly higher than that for C1-C3, indicating a weaker delay effect. It satisfies the hydrogeological conditions in C4-C6: active groundwater flow is limited in near-surface zone.

For the calibration period, the root-mean-square error (RMSE) of the 'natural' model for all of the catchments is 39% of the average monthly runoff. For annual runoff, the RMSE is 21% of the average annual runoff. The errors include the streamflow observation error and the meteorological data treatment error. It is more reasonable to evaluate the model according to the observation-simulation correlation coefficient and the NSE value. A comparison between the observed and simulated monthly runoff (including groundwater discharge) for all of the 6 catchments can be seen in Fig. 5. The coefficient of determination (R^2=0.89) is high. The NSE values of the model range between 0.48 and 0.81 (Table 3), not very high but close to or higher than 0.5, indicating that the model performs well in the study area. It is usually

difficult to obtain a high NSE value for a catchment with weak seasonal variation in runoff (Mathevet et al., 2006), such as that in C1 and C2.

4.2 Modelling results

We used this 'natural' model to estimate the monthly hydrological components during the whole 1957-2010 period. As an example, typical results of the HRC are shown in Fig. 6. The model estimates of monthly runoff after 1970s are generally higher than the observed values (Fig. 6a) due to ignoring the impacts of land use changes and increased utilization of water for irrigation. However, the simulated patterns of groundwater discharge are similar to the observations (Fig. 6b): falling in the summer, rising in the winter. This agreement between the simulated and observed patterns demonstrates the ability of the ABCD-GE model in simulating the hydrological behaviors in the studied catchment: significant groundwater-dependent evapotranspiration occurs in the summer, and a strong recovery of storage in the shallow-groundwater zone occurs in the winter due to delayed recharge from the thick vadose zone.

For the HRC, there are significant differences between the observed and model calculated annual runoff after 1966, as shown in Fig. 6c. This deviation could be interpreted as the excess evapotranspiration induced by increasing agricultural water use from river diversion. Enhanced, evapotranspiration also occurred in the shallow groundwater zone due to groundwater pumping for irrigation. To evaluate the actual water balance, the following equation:

$$E_{ACT} \approx E_{NAT} + (Q_{NAT} - Q_{OBS}) \qquad (18)$$

is applied to approximately estimate the actual annual evapotranspiration (E_{ACT}) after 1966 from the 'natural' model result (E_{NAT}) plus the difference of the annual runoff between the 'natural' model (Q_{NAT}) and the observation (Q_{OBS}). Thus, the irrigation water use in the catchment is included in E_{ACT}. Results are shown in Fig. 6d. It seems that the relative difference between E_{NAT} and E_{ACT} is not significant. The maximum $Q_{\mathrm{NAT}} - Q_{\mathrm{OBS}}$ value is less than 10% of the mean annual evapotranspiration (~315 mm). Accordingly, the irrigation water use in the HRC did not significantly influence the annual evapotranspiration at the catchment scale. However, it dramatically influenced the streamflow. As shown in Fig. 6a, almost all of the direct runoff was removed from the total runoff after 1987 and groundwater

discharge was significantly decreased even though the seasonal patterns basically remained (Fig. 6b).

4.3 Annual water balance in the standard Budyko space

In Fig. 7, the E/P data for the annual water balance obtained from the 'natural' model over the 1957-2010 period are plotted in the standard Budyko space. It is obvious that with the increasing aridity index ($\phi=E_0/P$), the evapotranspiration ratio ($F=E/P$) for all of the catchments increased in almost a linear trend with different slopes. When $\phi<4$, most of the data points fall below the original Budyko curve, indicating that F is generally less than 1.0 in this situation. When $\phi>4$, the original Budyko curve gives $F\approx1$, satisfying the limitation ($0<F\leq1$) for mean annual evapotranspiration ratio. However, some of the data points fall above the line of $F=1$ while ϕ is larger than 3 but even less than 4, indicating that the $F>1$ cases were not only occurred in extreme dry years. The maximum F value (2.2) was obtained in the HRC when the aridity index jumped from $\phi=1.5$ in 1964 to $\phi=9.8$ in 1965. It means that the HRC lost a volume of water in 1965 by evapotranpiration, which is more than twice of the gained water from precipitation in the same year. In comparison, the evapotranspiration ratios in C3 and C6 are not sensitive to the change in the aridity index since the slope of the F-ϕ trend is less than 0.1.

The effects of groundwater dependent evapotranspiration can be clearly observed when the evapotranspiration ratio is divided into two parts and plotted in the Budyko space separately with respect to the shallow and deep groundwater zones. The annual E values in the Zone-1 and Zone-2 are estimated, respectively, as:

$$E_1=\sum_{m=1}^{12}E_{1m}(W_{m-1},a,b) \quad \text{and} \quad E_2=\sum_{m=1}^{12}E_{2m}(G_m,g) \qquad (19)$$

for every year, where E_{1m} was calculated with Eq. (9), whereas E_{2m} was calculated with Eq. (14). Typical results are shown in Fig. 8 for the HRC (Fig. 8a) and C4 (Fig. 8b). The data in Fig. 8 were estimated with the parameter values of a, b and g for the 'natural' model. It is obvious that the annual E_1/P values in the Zone-1 (deep groundwater) for the whole range of the aridity index ($0<\phi<8$) are smaller than 1.0 and fall below the original Budyko curve determined by Eq. (2). The low E_1/P value in the Zone-1 is mainly due to the water limited condition in the soils without the supply of groundwater, especially in the HRC where the

landscape is dominated by sand dunes. The E_1/P trends can be approximately fitted by the Budyko curve determined with Eq. (3) using w =1.4 and 1.6, respectively, for the HRC and C4. The higher w value in C5 is linked with the higher b value of the model for C4, as listed in Table 3. However, the relationship between the annual evapotranspiration ratio and the annual aridity index in the shallow groundwater zone definitely could not be explained by any of the normal Budyko formulas, because for the Zone-2 all the annual F values are higher than 1.0 in the HRC (Fig. 8a) or most of the E_2/P data points fall above the bound in C4 (Fig. 8b).

In the HRC, the E_2/P data points follow a linear trend with the slope of 0.52 (Fig. 8a). This trend agrees with the relationship between E_2 and E_0 ($E_2 \propto E_0$) that described in Eq. (14). Since the groundwater storage, G, is relatively stable (small d and k values in the model), the annual E_2/P value would be proportional to the annual E_0/P value and the slope is close to the annual mean value of gG. In the HRC, the annual mean value of gG is 0.65 according to the 'natural' model. Such a groundwater dependent evapotranspiration process is the reason for the cases of $F>1$ occurred at the catchment scale in the HRC. Note that in the original Budyko framework, the $F=\phi$ case denotes an energy-limited condition when water supply (only precipitation for mean annual water balance) is sufficient for the evapotranspiration process. The slope of the E_2/P trend in Fig. 8a is less than 1 but is closer to the $F=\phi$ line than the water limited line represented by $F=1$. It indicates that in the Zone-2 the evapotranspiration process is in a quasi-energy limited condition, rather than in a water limited condition, because shallow groundwater can effectively serve as an external source of water supply.

In C4, the E_2/P data points show a scatter distribution around the correlation line for the trend (Fig. 8b). This is mainly caused by the significant variability in the groundwater storage, G, at the monthly and annual scales. The d and k values in the model for C4 are quite larger than that for the HRC by which the model could capture the significant fluctuation of baseflow. As a result, the annual mean gG value of C4 varied in a large range between 0.18 and 0.84. Similar unstable E_2/P data also exist for C5 and C6 as indicated by the high d and k values in the model for them (Table 3).

5 Discussions

5.1 Controls on the *F* >1 cases

It has been demonstrated in Fig. 7 that the annual evapotranspiration ratio, F, would be usually higher than 1.0 when the aridity index, ϕ, is larger than 4.0 in the studied catchments. In the literature, the F>1 cases were also observed when ϕ is just higher than 1.0 (Cheng et al., 2011; Wang, 2012; Chen et al, 2013). Thus, it is interesting to discuss how the occurrence of the F>1 cases is controlled by the catchment properties when shallow groundwater plays an important role.

The equation for the annual evapotranspiration ratio can be derived from Eqs. (15) and (19) as follows:

$$F = (1-\alpha)\frac{E_1}{P} + \alpha g \frac{E_0}{P}\sum_{m=1}^{12}\left(\frac{E_{0m}}{E_0}G_m\right) \quad (20)$$

where the term E_{0m}/E_0 denotes the proportion of monthly potential evaporation to the annual one with respect to the m-th month. It has been known that the relationship between E_1/P and ϕ determined by the ABCD model is similar to that predicted by the normal Budyko formulas, as shown in Fig. 8, where E_1/P is less than 1.0. For the groundwater dependent term, defining:

$$G_a = \sum_{m=1}^{12}\left(\frac{E_{0m}}{E_0}G_m\right) \quad (21)$$

as the weighted average of the monthly groundwater storage, Eq. (20) can be replaced by:

$$F(\phi) = (1-\alpha)[1+\phi-(1+\phi^w)^{1/w}] + \alpha g G_a \phi \quad (22)$$

where E_1/P is represented by Eq. (3). According to Eq. (22), the function $F(\phi)$ is controlled by the parameters, g, w, α and the status of groundwater represented by G_a. As indicated in Eq. (14), gG_a is a dimensionless parameter to describe the intensity of groundwater dependent evapotranspiration related to the potential evaporation. The recommended range of gG_a is 0.2-1.0 according to Table 3. In Eq. (22), the term of E_1/P indicates the normal energy-water limited process in Zone-1, whereas the term of groundwater indicates the quasi-energy limited process in Zone-2. The actual F value is a mixed result of the different processes.

Typical F-ϕ curves obtained with Eq. (22) are plotted in Fig. 9. It can be seen that the proportion of shallow water table area (α) has large effect on the occurrence of the F>1 case. When the shallow water table area is small (α=0.1), the F>1 case occurs only during extreme dry years. When groundwater dependent evapotranspiration (gG_a) increases, the case F>1 occurs with smaller aridity index. The specific catchment parameter (w) for E_1/P also influences the occurrence of the F>1 case. A larger w value shifts the F-ϕ curves (comparing Fig. 9b with Fig. 9a) to the left side indicating that the F>1 case could occur with smaller aridity index.

Groundwater dependent evapotranspiration estimated in the ABCD-GE model does not violate the F≤1 rule for the long-term mean annual water balance, because the model will yield E=P–Q for the average flux in a long-term period. As shown in Fig. 9, more than half of the data points fall below the line of F=1, indicating that the less-than-1 rule for the average F value is satisfied in the whole study area. For each catchment, in addition, the mean annual E/P versus E_0/P data for the 1957-2010 period has been shown in Fig. 8 (green cross lines). None of them is higher than 1.

5.2 Using effective precipitation and modified Budyko space

The standard Budyko space assumes that the potential water supply for evapotranspiration is only rainfall in a catchment. This is true for the long-term average water balance, but exceptions might exist for the annual or intra-annual behaviors. Wang (2012) and Chen et al. (2013) argued that the reduction of storage in a period should be regarded as one of the water supply components. They suggested an approach to replace the evapotranspiration ratio and the dryness index, respectively, by $E/(P-\Delta S)$ and $E_0/(P-\Delta S)$, where ΔS is the storage depletion in a studied period and $P-\Delta S$ regarded as the effective precipitation. In this modified Budyko space, evapotranspiration is always less than the water supply so that the original Budyko hypothesis could be applied for small time-scale problems. In this section, we attempt to check the characteristics of the annual water balance data in the study area using such a modified Budyko space. With the results of the ABCD-GE model, the total change in storage for a year can be estimated as:

$$\Delta S = \sum_{m=1}^{12}[(1-\alpha)(W_m + V_m - W_{m-1} - V_{m-1}) + (G_m - G_{m-1})] \qquad (23)$$

where m is the number of the months in the year, W_0, V_0 and G_0 for m=0 denoting the respective storage components at the end of the last year.

Results are shown in Fig. 10 for the 6 studied catchments. It can be seen that in the modified Budyko space the annual water balance data fall into the zone below the limitation: $E/(P-\Delta S)<1$. However, in any one of the cacthments, the shift path of the data points could not be captured by a single Budyko curve in the modified Budyko space. For the cases in C1 and C2, the rising trends of $E/(P-\Delta S)$ with the increasing $E_0/(P-\Delta S)$ seem too weak in comparison with any one of the normal Budyko curves determined by Eq. (3). Similar difference between the data trends and the normal Budyko curves also exist in the other catchments but not significant as that in C1 and C2. Furthermore, in C1 and C2 the $E/(P-\Delta S)$ value approaches a stable value around 0.90 with the high $E_0/(P-\Delta S)$ values. It indicates that at least 10% of $P-\Delta S$ is contributed to the annual runoff, in terms of $Q/(P-\Delta S)$. This portion of the water supply seems to be inaccessible for the annual evapotranspiration process. Such a bound of the $E/(P-\Delta S)$ value could also exist in C3-C6. In particular, this limitation is lower than 0.8 in C3, implying significant contribution of change in storage on the streamflow in drought years.

The difficulties in using the effective precipitation defined by Wang (2012) and Chen et al. (2013) are the unkown ΔS for an investigated time step and the possible existence of the inaccessible part of ΔS for evapotranspiration. Consequently, the estimation of $E/(P-\Delta S)$ value is not straightforward, but requires a complex iteration process. In the original Budyko framework for the steady state water balance, the water supply (only precipitation) does not depend on both evapotranspiration and runoff so that the aridity index is an independent variable in assessing the behaviors of the catchments. However, the water supply represented by the effective precipitation is influenced by the evapotranspiration-runoff processes due to the feedback mechanism. This cross-dependency between the water supply and evapotranspiration significantly reduces the efficiency of using the modified Budyko space in analyzing the shift of annual water balance in a catchment. In contrast, it would be an efficient and straightforward approach to extend formulas for annual water balance in the standard Budyko space, such as Eq. (22), keeping an independent index (ϕ) for the climatic conditions.

5.3 Landscape-driven and human-controlled shifts of annual water balance

As illustrated in Fig. 6d, the actual evapotranspiration in the HRC has been enhanced by human activities. This impact might exist in both the shallow and deep groundwater zones. Crops in the HRC are mainly planted in the depressions and terrace lands with shallow groundwater, especially in the river valley. Crops require much more water than the precipitation for growing. For example, maize could consume more than 3 times of rainfall water in growing seasons (Zhou et al., 2013). Thus, irrigation is necessary to maintain the agricultural production. In the farmlands far away from the rivers, groundwater was abstracted from wells for irrigation. In the river valley, irrigation was realized with diversions and channels. Therefore, an increase in evapotranspiration in the shallow groundwater zone is dominated by irrigation. Along the river, the area of the surface water body was significantly enlarged in reservoirs leading to increase in surface water evapotranspiration loss. It is equivalent to increase in groundwater dependent evapotranspiration in this study because surface water is also included in the shallow groundwater zone. As a result, the shift of the annual water balance in the Budyko space was partly caused by change in land use and controlled by regulation of river water for irrigation.

Recently, Jaramillo and Destouni (2014) developed a method to assess the landscape-driven change in the mean evapotranspiration ratio using the difference between the actual change in the F value and the climate-driven change in the F value following the Budyko framework. In this section, we extend their method to assess the landscape-driven change in annual water balance in the HRC. The period between 1957-1966 is selected from Table 2 as the reference period. Changes are evaluated for the different average values of the annual E/P data in the different periods listed in Table 2. The climate-driven change is estimated with the annual E_{NAT} values obtained from the 'natural' model, using a formula similar to Jaramillo and Destouni (2014), as follows:

$$\Delta\left(\frac{E_{LD}}{P}\right)=\Delta\left(\frac{E_{ACT}}{P}\right)-\Delta\left(\frac{E_{NAT}}{P}\right) \qquad (24)$$

where $\Delta(E_{LD}/P)$ denotes the landscape-driven change in comparison with the 1957-1966 period. However, this quantity index includes the landscape changes driven by both climatic force and human activities. To check how this index is correlated with the increasing impacts from the reservoirs and diversions in rivers, following Jaramillo and Destouni (2015), the

intra-annual variability of the monthly runoff (CV_Q) was applied. The CV_Q/CV_P value was estimated to reveal the separate influence of such a human-controlled flow regulation from the mixed human-climate controlling, where CV_P is the intra-annual variability of the monthly rainfall.

Results of the $\Delta(E_{LD}/P)$ and $\Delta(CV_Q/CV_P)$ data between the three periods 1968-1987, 1988-1997, 1998-2010 and the reference period 1957-1967 are shown for the HRC in Fig. 11. The $\Delta(E_{LD}/P)$ values are all positive but not big (less than 6%), indicating a slight increase in the evapotranspiration ratio after 1966 driven by changes in natural landscape conditions of water storage and/or human controlled land use. The $\Delta(CV_Q/CV_P)$ values show a significant fluctuation around zero but also limited in a small range (±5%). Both the $\Delta(E_{LD}/P)$ and $\Delta(CV_Q/CV_P)$ values are largest in 1988-1997. Fluctuations of these data could not be fully explained by the increasing number of diversions in the rivers. The negative $\Delta(CV_Q/CV_P)$ value in 1968-1987 may be caused by construction of the two reservoirs since reservoirs commonly smooth the variation of streamflow. In 1988-1997, the $\Delta(CV_Q/CV_P)$ value turned to positive when 5 new diversions was built, indicating the opposite impacts of the reservoirs and diversions. It is possible that the streamflow was disturbed by the regulation of water for irrigation on these diversions with small overflow dams. Decrease in the $\Delta(CV_Q/CV_P)$ value from 4.72% in 1988-1977 to 0.72% in 1998-2010 may be caused by the control of river water use under some government policies to prevent the desertification (Yang et al., 2012; Zhou et al., 2015). The following decrease in the $\Delta(E_{LD}/P)$ value form 5.05% in 1988-1997 to 3.73% in 1998-2010 is not significant, seems indicating alternative irrigation practice in farmlands (for example pumping groundwater) so that the real water consumption was reduced but still on a high level. As a result, utilization of surface water and groundwater for irrigation can increase the frequency of the $F>1$ cases.

5.4 Limitation Remarks

Attention should be paid to the simplifications in the conceptual model extended from the ABCD model, when the equations and formulas are applied in complicated catchments. The ABCD model assumes that the storage-evapotranspiration relationship is controlled by the parameters *a* and *b* whereas the physical interpretation of them is difficult (Alley, 1984). Equation (8) in the ABCD model is also hypothesized from a simplified storage-loss process that controlled by the parameter *b* (Thomas, 1981). Sankarasubramanian and Vogel (2002)

suggested that the b value for annual water balance could be approximately represented by the maximum soil moisture field capacity plus maximum E_0 for ϕ<1 or maximum P for ϕ≥1. The a value is generally estimated in a small range between 0.95 and 1.0. In this study, the model output is not sensitive to the a value. The correlation between a and b may exist because both of them are positively related with E_m+W_m in Eq. (7). The ABCD model neglects the possibility of groundwater-dependent evapotranspiration which has been incorporated in the ABCD-GE model. The ABCD-GE model divides the area into shallow and deep groundwater zones, without considering a complicated spatial distribution of groundwater depth. For the shallow groundwater zone, the evapotranspiration is assumed to be proportional to the groundwater storage. Nonlinear behavior in groundwater dependent evapotranspiration could be further included if it can be successfully parameterized. Linear groundwater storage-discharge relationship is adopted in both of the ABCD and ABCD-GE models. These simplifications could cause systematic errors in modeling a catchment where the nonlinear behaviors in the hydrological processes are significant.

In fact, when the Budyko framework is applied for small time-scale water balance in a catchment, the other additional sources of water supply should be considered, apart from groundwater. Significant changes in soil moisture, snow cover or frozen water in cold regions could also cause 'abnormal' shift of annual water balance for a catchment in the standard Budyko space (Jaramillo and Destouni, 2014). The effects of these storage components are negligible in this study but may be essential in other study areas. In particular, the special processes in cold regions are not included in the ABCD-GE model. However, one can refer to Martinez and Gupta (2010) who proposed the snow-augmented ABCD model, which is easy to be incorporated into an extension of the ABCD-GE model.

6 Conclusions

The Budyko framework was developed for long-term mean annual water balance in catchments, which estimates the evapotranspiration ratio (F) as a function of the aridity index (ϕ). It can be represented by curves for the F-ϕ relationship in the standard Budyko space that were determined by the original Budyko formula without any parameter or formulas with a catchment specific parameter. It is interesting to investigate whether the Budyko space can be also applied to capture the annual water balance in a catchment with varying dryness.

However, the shift of annual water balance in the standard Budyko space could be significantly different from that presumed from the normal Budyko curves, in particular, when the cases of $F>1$ occur as that have been observed in a number of catchments.

In this study, we highlighted the effects of groundwater dependent evapotranspiration in triggering the abnormal shift of annual water balance in the standard Budyko space. A conceptual monthly hydrological model, the ABCD-GE model, was developed from the widely used ABCD model to incorporate the groundwater-dependent evapotranspiration in the zone with shallow water table and delayed groundwater recharge in the zone with deep water table. The model was successfully applied to analyze the shift of annual water balance in 6 catchments in the Erdos Plateau, China.

The results show that the normal Budyko formulas are not applicable for the interannual variability of catchment water balance when groundwater dependent evapotranspiration is significant. The shift of annual water balance in the F-ϕ space is a combination of the Budyko-type response in the deep groundwater zone and the quasi-energy-limited condition in the shallow groundwater zone. Shallow groundwater supplies excess evapotranspiration during drought years, leading to the $F>1$ cases. The occurrence of the $F>1$ cases depends on the proportion area of the shallow groundwater zone, the intensity of groundwater dependent evapotranspiration and the catchment properties determining the Budyko-type trend in the deep groundwater zone. Water utilization for irrigation may enhance this excess evapotranspiration phenomenon. The modified Budyko space with the effective precipitation incorporating the change in storage can force F values below 1.0. However, the computation is complicated in dealing with the feedback between the water supply and evapotranspiration loss as well as the existence of inaccessible storage for evapotranspiration. The empirical formula proposed in this study for the standard Budyko space provides a straightforward method to predict the trend of annual water balance with the varying dryness.

Acknowledgements

This study is supported by the Program for New Century Excellent Talents in University (NCET) that granted by the Ministry of Education, China, and partly supported by the Honor Power Foundation, UNESCO-IHE. The authors are grateful to the constructive comments

from Dr. Donohue, Dr. Jaramillo and an anonymous reviewer which helped to improve the manuscript.

References

Arora, V. K.: The use of the aridity index to assess climate change effect on annual runoff, J. Hydrol., 265, 164-177, 2002.

Alley, W. M.: On the treatment of evapotranspiration, soil moisture accounting, and aquifer recharge in monthly water balance models, Water Resour. Res., 20, 1137–1149, 1984.

Budyko, M. I.: Evaporation under natural conditions, Isr. Program for Sci. Transl., Jerusalem, 1948.

Budyko, M. I.: The heat balance of the earth's surface, U.S. Department of Commerce, Washington, D. C., U.S.A., 1958.

Budyko, M. I.: Climate and life, Academic, New York, U.S.A., 1974.

Chen, X., and Hu, Q.: Groundwater influences on soil moisture and surface evaporation, J. Hydrol., 297, 285–300, 2004.

Cheng, L., Xu, Z., Wang, D., and Cai, X.: Assessing interannual variability of evapotranspiration at the catchment scale using satellite-based evapotranspiration data sets, Water Resour. Res., 47, W09509, doi:10.1029/2011WR010636, 2011

Chen, X., Alimohammadi, N., and Wang D.: Modeling interannual variability of seasonal evaporation and storage change based on the extended Budyko framework, Water Resour. Res., 49, 6067–6078, doi:10.1002/wrcr.20493, 2013

Cohen, D., Person, M.,Daannen, R.,Sharon, L.,Dahlstrom, D., Zabielski, V., Winter, T.C., Rosenberry, D.O., Wright, H.,Ito, E., Nieber, J.,and Gutowski Jr, W.J: Groundwater-supported evapotranspiration within glaciated watersheds under conditions of climate change. J. Hydrol., 320, 484–500, 2006.

Fan, J., Wang, Q., and Hao, M.: Estimation of reference crop evapotranspiration by Chinese pan, Transactions of the CSAE, 22(7), 14-17, 2006. (in Chinese)

Fernandez, W., Vogel, R. M. and Sankarasubramanian A.: Regional calibration of a watershed model, Hydrol. Sci. J., 45, 689–707, 2000.

Fu, B. P.: On the calculation of the evaporation from land surface, Sci. Atmos. Sin., 5, 23-31, 1981. (in Chinese)

Gerrits, A. M. J., Savenije ,H. H. G., Veling, E. J. M., and Pfister, L.: Analytical derivation of the Budyko curve based on rainfall characteristics and a simple evaporation model, Water Resour. Res., 45, W04403, 2009. doi: 10.1029/2008wr007308.

Greve, P., Gudmundsson, L.,Orlowsky, B., and Seneviratne, S. I.: Introducing a probabilistic Budyko framework, Geophysical Research Letters, 42: 2261-2269, 2015.

Istanbulluoglu, E., Wang, T. Wright, O. M. and Lenters, J. D.: Interpretation of hydrologic trends from a water balance perspective: The role of groundwater storage in the Budyko hypothesis, Water Resour. Res., 48, W00H16, 2012. doi:10.1029/2010WR010100.

Jaramillo,F. and Destouni, G.: Developing water change spectra and distinguishing change drivers worldwide. Geophys. Res. Lett., 41, 8377–8386, 2014.

Jaramillo, F., and Destouni, G.: Local flow regulation and irrigation raise global human water consumption and footprint. Science 350, 1248–1251, 2015.

Li, W. and Sankarasubramanian, A.: Reducing hydrologic model uncertainty in monthly streamflow predictions using multimodel combination, Water Resour. Res., 48, W12516, 2012. doi:10.1029/2011WR011380.

Lv, J., Wang, X.-S., Zhou, Y., Qian, K., Wan, L., Derek, E., and Tao Z.: Groundwater-dependent distribution of vegetation in Hailiutu River catchment, a semi-arid region in China, Ecohydrology, 2013, 6: 142-149, 2013.

Mathevet, T., Michel, C., Andreassian, V.and Perrin C.: A bounded version of the Nash-Sutcliffe criterion for better model assessment on large sets of basins, In: Large Sample Basin Experiments for Hydrological Model Parameterization: Results of the Model Parameter Experiment–MOPEX, IAHS Publ. 307, p.211-218, 2006.

Martinez, G. F., and Gupta, H. V.: Toward improved identification of hydrological models: A diagnostic evaluation of the ‘‘abcd’’ monthly water balance model for the conterminous United States, Water Resour. Res., 46, W08507, 2010. doi:10.1029/2009WR008294

Mezentsev, V. S.: More on the calculation of average total evaporation, Meteorol. Gidrol., 5, 24–26, 1955.

Middleton, N. and Thomas, D. S. G. (Eds.): World atlas of desertification, United Nations Environment Programme, Edward Arnold, 1992.

Nash, J. E. and Sutcliffe, J. V.: River flow forecasting through conceptual models part I — A discussion of principles, J. Hydrol., 10 (3), 282–290, 1970.

Porporato, A., Daly, E. and Rodriguez-Iturbe, I.: Soil water balance and ecosystem response to climate change, American Naturalist, 164, 625-632, 2004.

Potter, N. J., and Zhang, L.: Interannual variability of catchment water balance in Australia, J. Hydrol., 369, 120–129, 2009.

Renner, M., Seppelt, R. and Bernhofer, C.: Evaluation of water-energy balance frameworks to predict the sensitivity of streamflow to climate change, Hydrol. Earth Syst. Sc., 16, 1419-1433, 2012.

Roderick, M. L., and Farquhar, G. D.: A simple framework for relating variations in runoff to variations in climatic conditions and catchment properties, Water Resour. Res., 47, W00G07, 2011. doi: 10.1029/2010WR009826.

Sankarasubramanian, A., and Vogel, R. M.: Annual hydroclimatology of the United States, Water Resour. Res.,38, 1083, 2002. doi:10.1029/2001WR000619.

Shi, C., Niu, K. Chen, T. and Zhou, X.: The study of pan coefficients of evaporation pans, Scientia Gepgrophica Sinica, 6(4), 305-313, 1986. (in Chinese)

Sloto, R. A. and Crouse, M. Y.: HYSEP: a computer program for streamflow hydrograph separation and analysis, US Geological Survey Water-Resources Investigations Report 96-4040, 1996.

Thomas, H. A.: Improved methods for national water assessment, report, Contract WR 15249270, U.S. Water Resour. Council, Washington, D. C.,1981.

Vandewiele, G. L., Xu, C.-Y. and Ni-Lar-Win: Methodology and comparative study of monthly water balance models in Belgium, China and Burma, J. Hydrol., 134, 315–347, 1992.

Wang, D.: Evaluating interannual water storage changes at watersheds in Illinois based on long-term soil moisture and groundwater level data, Water Resour. Res., 48, W03502, 2012. doi:10.1029/2011WR010759.

Wang, D., and Tang, Y.: A one-parameter Budyko model for water balance captures emergent behavior in darwinian hydrologic models, Geophys. Res. Lett., 41, 4569–4577, 2014. doi:10.1002/2014GL060509.

Wang, T., Istanbulluoglu, E., Lenters, J. and Scott D.: On the role of groundwater and soil texture in the regional water balance: An investigation of the Nebraska Sand Hills, USA, Water Resour. Res., 45, W10413, 2009. doi:10.1029/2009WR007733.

Yang, D., Shao, W., Yeh, P. J. F., Yang, H., Kanae, S., and Oki, T.: Impact of vegetation coverage on regional water balance in the nonhumid regions of China, Water Resour. Res., 45, W00a14, 2009. doi: 10.1029/2008wr006948.

Yang, D., Sun, F., Liu, Z., Cong, Z. and Lei Z.: Interpreting the complementary relationship in non-humid environments based on the Budyko and Penman hypotheses, Geophys. Res. Lett., 33(18), L18402, 2006. doi: 10.1029/2006gl027657.

Yang, D., Sun, F., Liu, Z., Cong, Z., Ni, G., and Lei Z.: Analyzing spatial and temporal variability of annual water-energy balance in nonhumid regions of China using the Budyko hypothesis, Water Resour. Res., 43(4), W04426, 2007. doi: 10.1029/2006wr005224.

Yang, H., Yang, D., Lei, Z., and Sun, F.: New analytical derivation of the mean annual water-energy balance equation, Water Resour. Res., 44, W03410, 2008. doi: 10.1029/2007WR006135.

Yang, Z., Zhou, Y., Wenninger, J. and Uhlenbrook, S.: The causes of flow regime shifts in the semi-arid Hailiutu River, Northwest China, Hydrol. Earth Syst. Sc., 16, 87-103, 2012.

Yeh, P. J.-F., and Famiglietti J. S.: Regional Groundwater Evapotranspiration in Illinois. Journal of Hydrometeorology, 10, 464-478, 2009.

Yin, L., Zhou, Y., Huang, J., Wenninger, J., Zhang, E., Hou, G., and Dong, J.: Interaction between groundwater and trees in an arid site: Potential impacts of climate variation and groundwater abstraction on trees, J. Hydrol., 528,435–448, 2015.

York, J.P., Person, M., Gutowski, W.J. and Winter, T.C.: Putting aquifers into atmospheric simulation models: An example from the Mill Creek Watershed, Northeastern Kansas, Advances in Water Resources, 25, 221–238, 2002.

Zhang, L., Dawes, W. R. and Walker G. R.: Response of mean annual evapotranspiration to vegetation changes at catchment scale, Water Resources Research, 37(3), 701-708, 2001. doi: 10.1029/2000wr900325.

Zhang, L., Hickel, K., Dawes, W. R., Chiew, F. H. S., Western, A. W. and Briggs P. R.: A rational function approach for estimating mean annual evapotranspiration, Water Resources Research, 40, W02502, 2004. doi: 10.1029/2003WR002710.

Zhang, L., Potter, N., Hickel, K., Zhang, Y. and Shao, Q.: Water balance modeling over variable time scales based on the Budyko framework - Model development and testing, Journal of Hydrology, 360(1-4), 117-131, 2008. doi: 10.1016/j.jhydrol.2008.07.021.

Zhou, Y., Wenninger, J., Yang, Z., Yin, L., Huang, J., Hou, L., Wang, X., Zhang, D., and Uhlenbrook, S.: Groundwater–surface water interactions, vegetation dependencies and implications for water resources management in the semi-arid Hailiutu River catchment, China – a synthesis, Hydrology and Earth System Sciences, 17, 2435–2447, 2013.

Zhou, Y., Yang, Z., Zhang, D., Jin, X., and Zhang, J.,: Inter-catchment comparison of flow regime between the Hailiutu and Huangfuchuan rivers in the semi-arid Erdos Plateau, Northwest China, Hydrological Sciences Journal, 60(4), 688-705, 2015.

1 Table 1. The characteristics of the study catchments shown in Fig. 1.

Catchments	Area (km^2)	Mean annual Flux[†]			
		P (mm)	E_0 (mm)	Q (mm)	Baseflow Index
C1	2645	367	1245	37.7	0.88
C2	2415	386	1218	38.8	0.64
C3	3253	447	1162	127.2	0.72
C4	3065	381	1227	75.8	0.31
C5	1272	466	1146	81.8	0.13
C6	3246	412	1186	53.0	0.16

2 [†] According to the data in the 1957-1978 period.

3

4

Table 2. Mean annual fluxes in the Hailiutu River catchment (HRC) in different periods

Periods	P(mm)	E_0(mm)	Q(mm)	Number Of Diversions(reservoirs)[†]
1957-1966	387.0	1230.2	42.3	0(0)
1967-1987	337.0	1269.6	32.6	4(2)
1988-1997	329.9	1240.2	23.4	9(2)
1998-2010	352.8	1234.0	28.0	10(2)

[†] According to Yang et al. (2012).

Table 3. Best fitting parameters of the 'natural' model for the study catchments.

Catchments	*a*	*b* (mm)	*c*	*d*	g	*k*	α	$\alpha g G_{mean}$ †	NSE
C1	0.97	33	0.97	0.05	0.010	0.017	0.21	0.14	0.51
C2	0.91	75	0.92	0.11	0.058	0.025	0.09	0.12	0.43
C3	0.91	41	0.90	0.18	0.017	0.017	0.18	0.15	0.71
C4	0.94	83	0.68	0.19	0.049	0.076	0.21	0.09	0.67
C5	0.97	155	0.67	0.10	0.070	0.214	0.27	0.14	0.81
C6	0.93	179	0.67	0.11	0.077	0.162	0.18	0.11	0.71

† G_{mean} is the mean value of the effective groundwater storage in the calibration period

Figure Captions:

Figure 1. Geographic information of the study site: (a) location of the study area in north central China; (b) Distribution of meteorological stations in the Erdos Plateau (green points) and contours of mean annual precipitation plotted from 1-km resolution gridded precipitation data; (c) Characteristics of landscape in the Hailiutu River Catchment (HRC) according to Lv et al. (2013). C1-C6 are the study catchments where C1 is the HRC.

Figure 2. The monthly meteorological data (a) and streamflow-baseflow data (b) from 1957 to 2010 in the HRC.

Figure 3. The plots of the annual $(P-Q)/P$ data versus the aridity index in the study catchments for the 1957-1978 period: (a) the mean annual data points for the 6 catchments bounded by the two Budyko curves (dashed lines) according to Eq. (3) with w=1.6 and w=2.5; and (b)-(f) are the annual data points of different catchments. C1-C6 are the numbers of the catchments shown in Fig. 1. The solid line is the original Budyko curve determined with Eq. (2). The dashed lines are the regression curves of the scatter data points with the slope values shown nearby.

Figure 4. Schematic representations of the ABCD model (a) and ABCD-GE model (b). W and V are the effective soil water storage and the effective storage in the transition vadose zone, respectively. G is the effective groundwater storage.

Figure 5. Scatter plot of the observed and simulated monthly runoff (mm) data (including groundwater discharge) of all the study catchments for the calibration period.

Figure 6. Simulated results of the ‘natural’ ABCD-GE model in comparison with the observation data in the HRC from 1957 to 2010, including: Monthly runoff (a), groundwater discharge (b), annual runoff (c) and annual evapotranspiration (d). The actual evapotranspiration in (d) was estimated with Eq. (18).

Figure 7. Plots of the annual evapotranspiration ratio in the study catchments versus the annual aridity index in the standard Budyko space for the 1957-2010 period. The actual evapotranspiration is estimated using the 'natural' model. The solid blue line is the original Budyko curve determined with Eq. (2). The dashed red lines are the linear regression curves of the data points with the slope data shown nearby. The intersection point of the green lines denotes the mean annual data.

Figure 8. Plots of the F-ϕ data in the standard Budyko space using the E_1 data for the Zone-1 and the E_2 data for the Zone-2 that estimated with Eq. (19): (a) in the HRC; (b) in C4. The red curves are the Budyko curves determined with Eq. (3), which could approximately represent the trends of the E_1/P data. The dashed blue lines are the linear regression curves of the E_2/P data.

Figure 9. The typical F-ϕ curves for annual water balance in the standard Budyko space determined with Eq. (22) when w=1.5 (a) and w=2.0 (b). The solid and dashed curves are estimated using gG_a=0.2 and gG_a=1.0, respectively. Dots are the data points of the 6 study catchments.

Figure 10. Annual water balance data in the modified Budyko space with the effective precipitation defined by Wang (2012). Dots are the data obtained for the catchments using the ‘natural’ model. The solid curves represents the normal Budyko curves determined with Eq.(3) using $E_0/(P-\Delta S)$ and $E/(P-\Delta S)$, respectively, instead of F and ϕ. w=1.9 and w=2.5 were selected to bound the data points of the HRC and applied for the comparison with the other catchments. The dashed lines approximately represent the actual bound of the $E/(P-\Delta S)$ data.

Figure 11. Historgram of the $\Delta(E_{LD}/P)$ data determined with Eq. (24) and the $\Delta(CV_Q/CV_P)$ data determined with the intra-annual variability of the monthly runoff (CV_Q) and rainfall (CV_P) for the different periods in the HRC. The numbers of diversions (reservoirs) are shown on the top of the blocks according to Table 2.

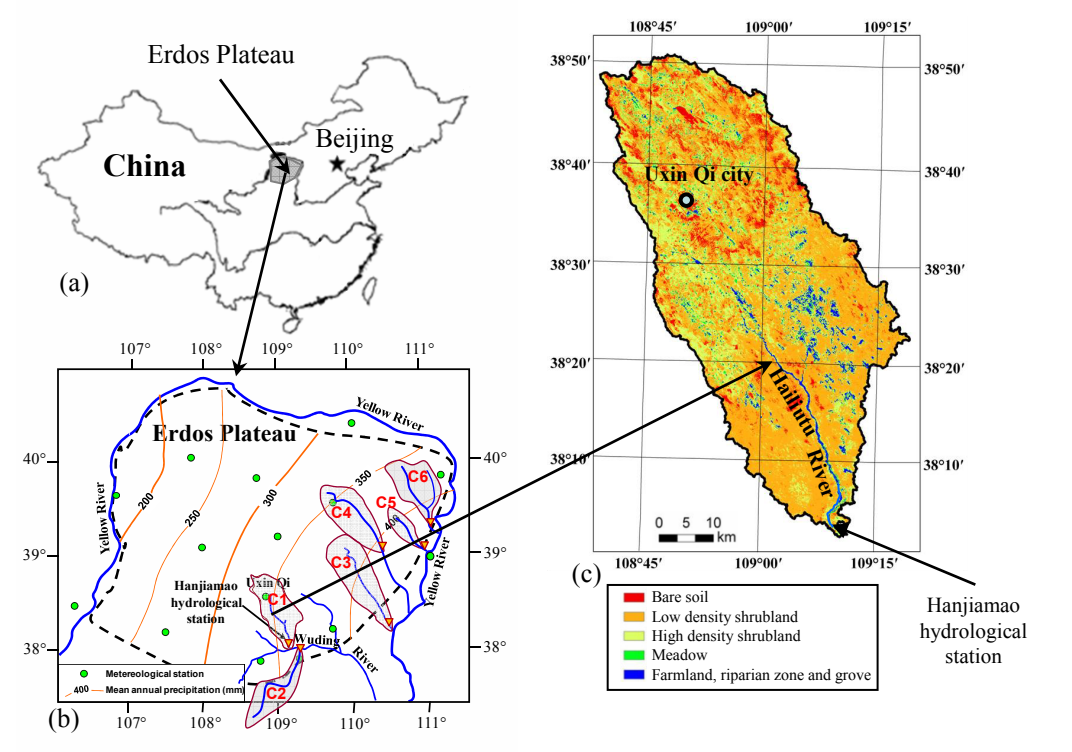
Erdos Plateau
China
Beijing
(a)
107°
108°
109°
110°
111°
40°
39°
38°
Erdos Plateau
Yellow River
Yellow River
Yellow River
200
250
300
350
400
C1
C2
C3
C4
C5
C6
Hanjiamao hydrological station
Uxin Qi
Wuding River
Metereological station
Mean annual precipitation (mm)
(b)
108°45′
109°00′
109°15′
38°50′
38°40′
38°30′
38°20′
38°10′
Uxin Qi city
Hailiutu River
0 5 10 km
(c)
Bare soil
Low density shrubland
High density shrubland
Meadow
Farmland, riparian zone and grove
Hanjiamao hydrological station

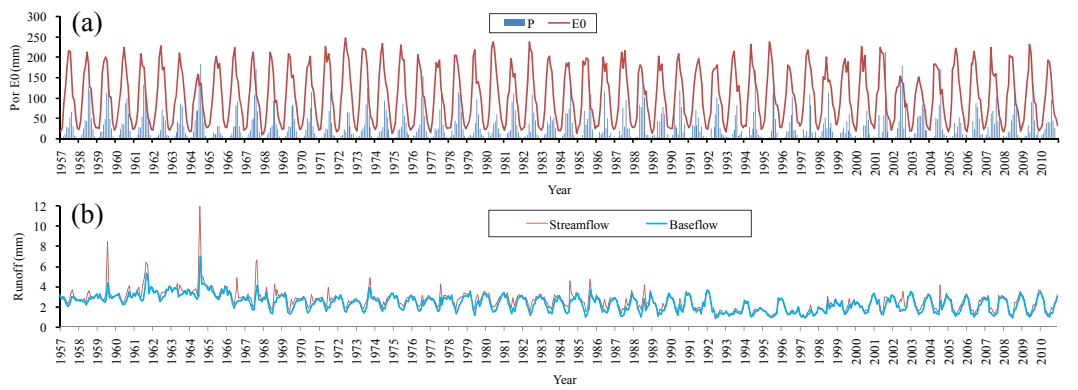
(a)
P
E0
Por E0(mm)
300
250
200
150
100
50
0
1957
1958
1959
1960
1961
1962
1963
1964
1965
1966
1967
1968
1969
1970
1971
1972
1973
1974
1975
1976
1977
1978
1979
1980
1981
1982
1983
1984
1985
1986
1987
1988
1989
1990
1991
1992
1993
1994
1995
1996
1997
1998
1999
2000
2001
2002
2003
2004
2005
2006
2007
2008
2009
2010
Year
(b)
Streamflow
Baseflow
Runoff(mm)
12
10
8
6
4
2
0
1957
1958
1959
1960
1961
1962
1963
1964
1965
1966
1967
1968
1969
1970
1971
1972
1973
1974
1975
1976
1977
1978
1979
1980
1981
1982
1983
1984
1985
1986
1987
1988
1989
1990
1991
1992
1993
1994
1995
1996
1997
1998
1999
2000
2001
2002
2003
2004
2005
2006
2007
2008
2009
2010
Year

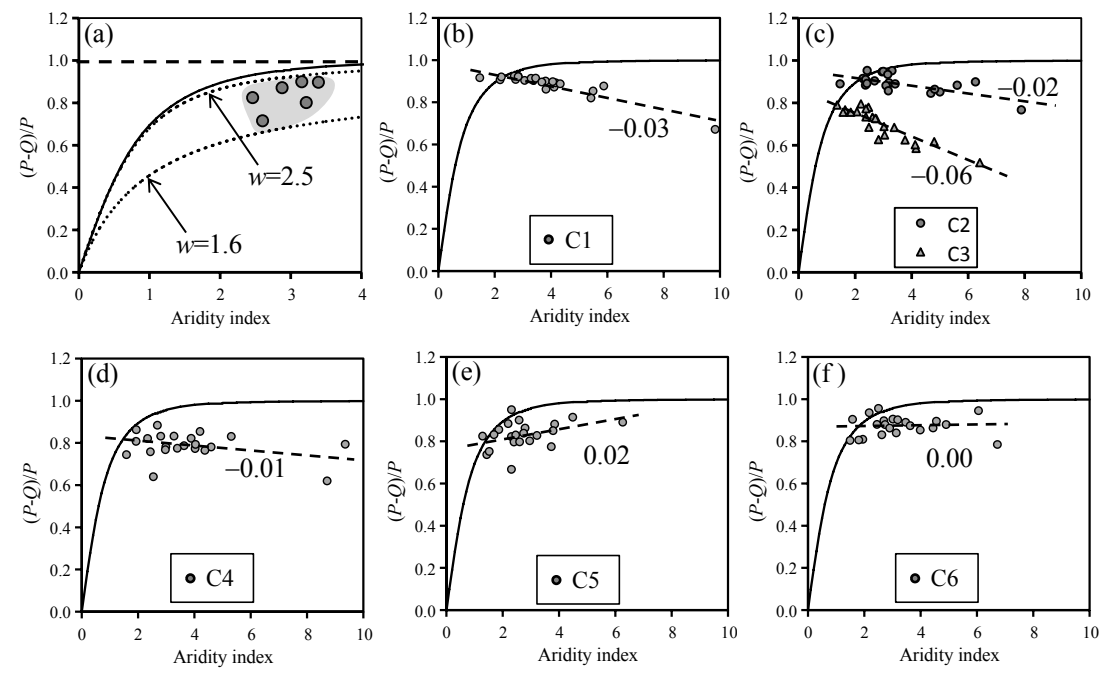
(a)
(P-Q)/P
Aridity index
w=2.5
w=1.6
(b)
–0.03
C1
(c)
–0.02
–0.06
C2
C3
(d)
–0.01
C4
(e)
0.02
C5
(f)
0.00
C6

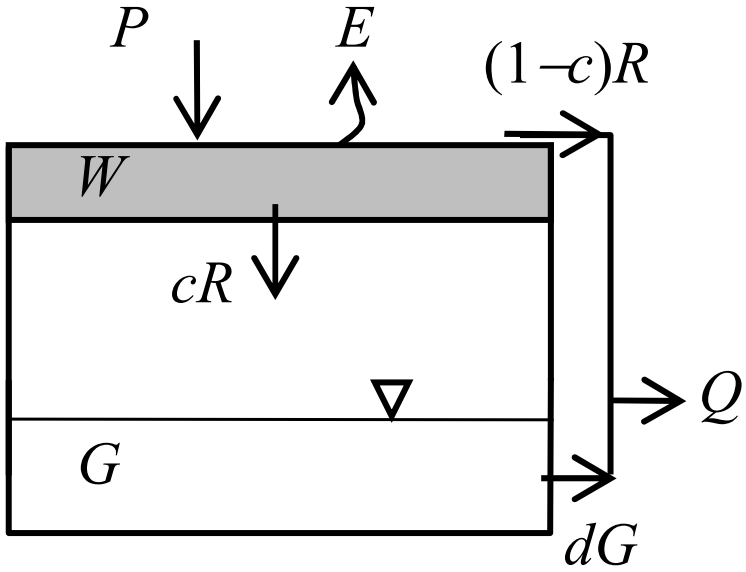

(a)

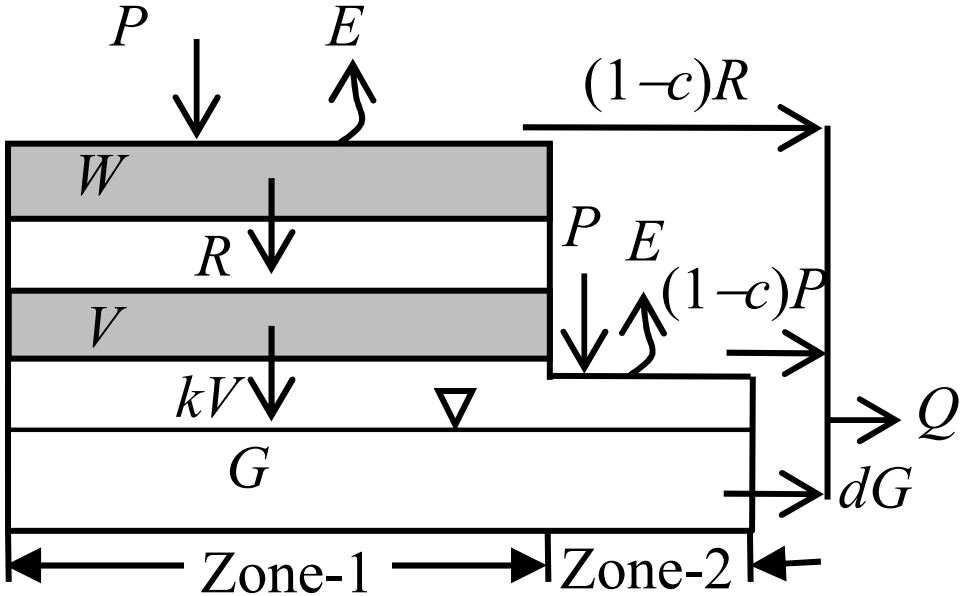

(b)

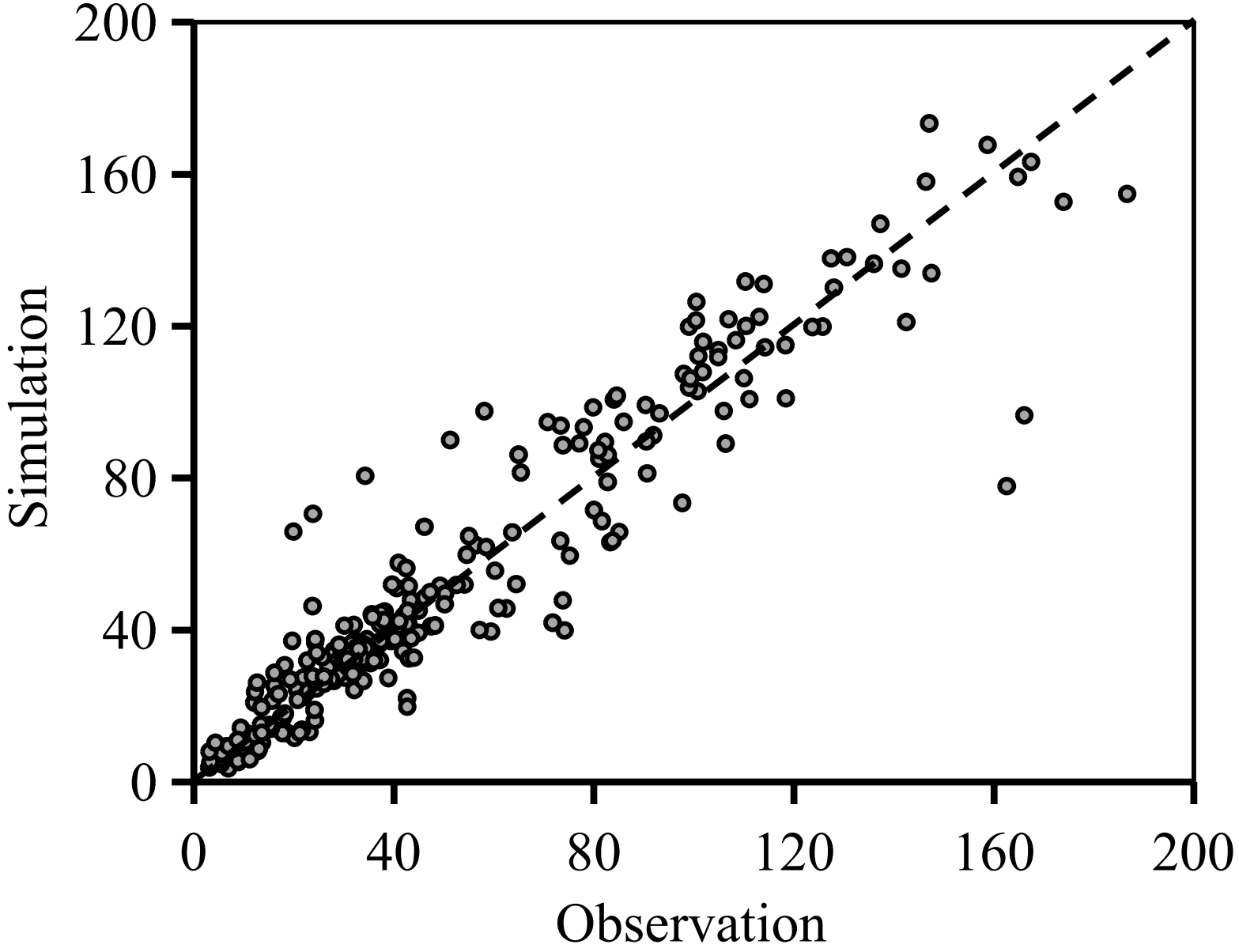
200
160
120
80
40
0
Simulation
0
40
80
120
160
200
Observation

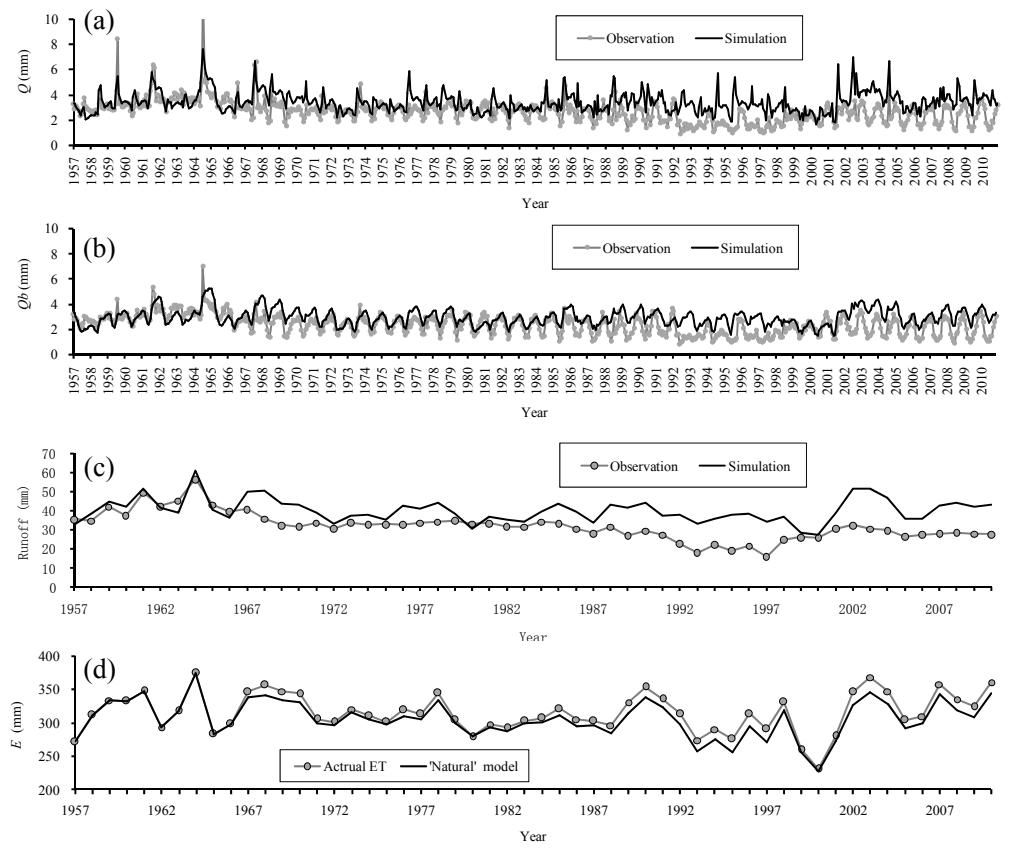
(a)
Observation
Simulation
Q (mm)
Year
(b)
Observation
Simulation
Qb (mm)
Year
(c)
Observation
Simulation
Runoff (mm)
Year
(d)
Actrual ET
'Natural' model
E (mm)
Year

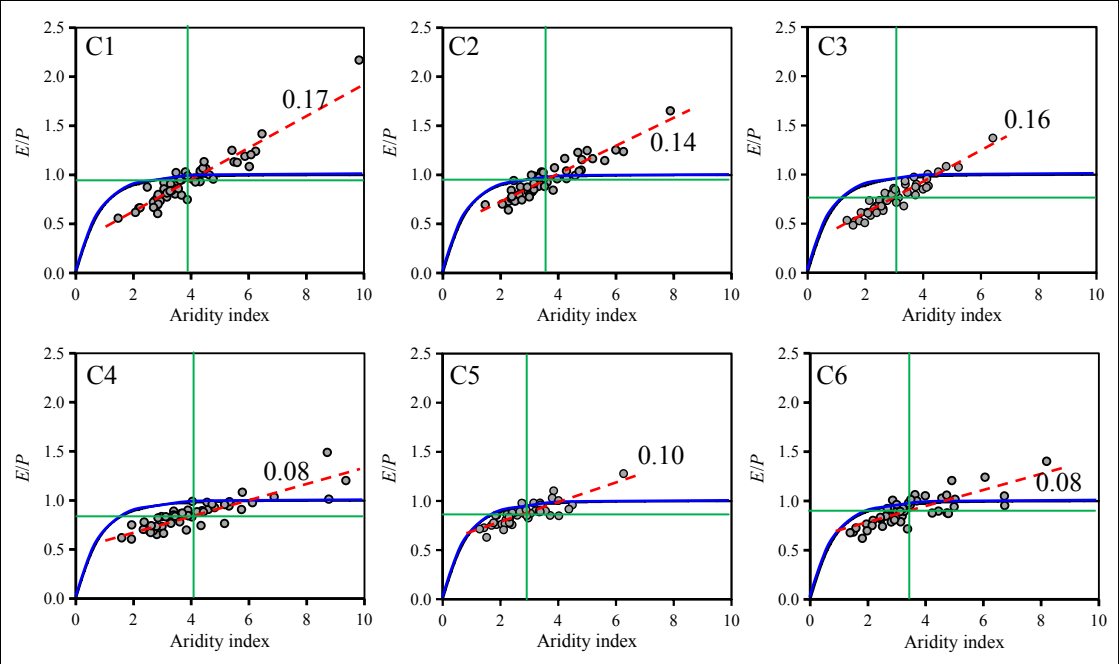
C1
0.17
C2
0.14
C3
0.16
C4
0.08
C5
0.10
C6
0.08
E/P
Aridity index
0.0
0.5
1.0
1.5
2.0
2.5
0
2
4
6
8
10

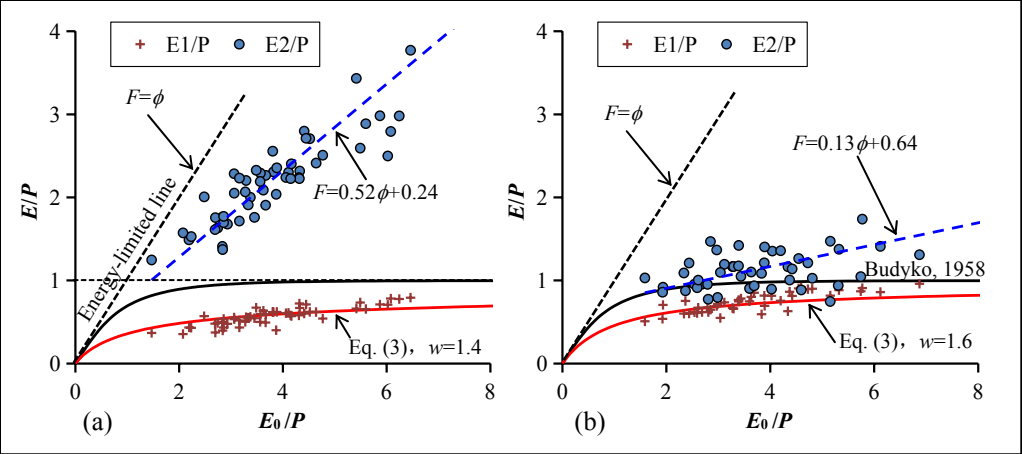
E1/P
E2/P
F=ϕ
Energy-limited line
F=0.52ϕ+0.24
Eq. (3), w=1.4
E/P
E0/P
(a)
E1/P
E2/P
F=ϕ
F=0.13ϕ+0.64
Budyko, 1958
Eq. (3), w=1.6
E/P
E0/P
(b)

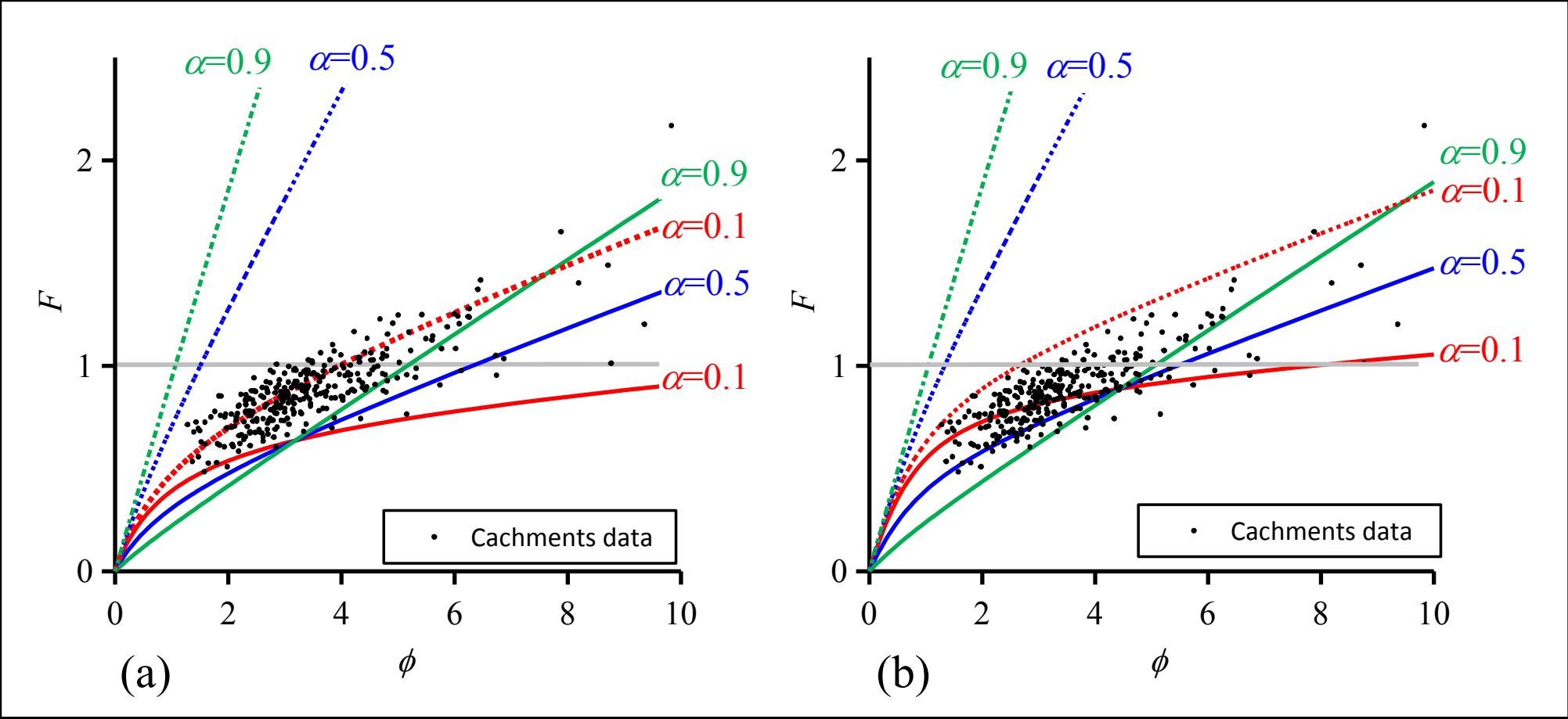
α=0.9
α=0.5
α=0.9
α=0.1
α=0.5
α=0.1
F
ϕ
Cachments data
(a)
α=0.9
α=0.5
α=0.9
α=0.1
α=0.5
α=0.1
F
ϕ
Cachments data
(b)

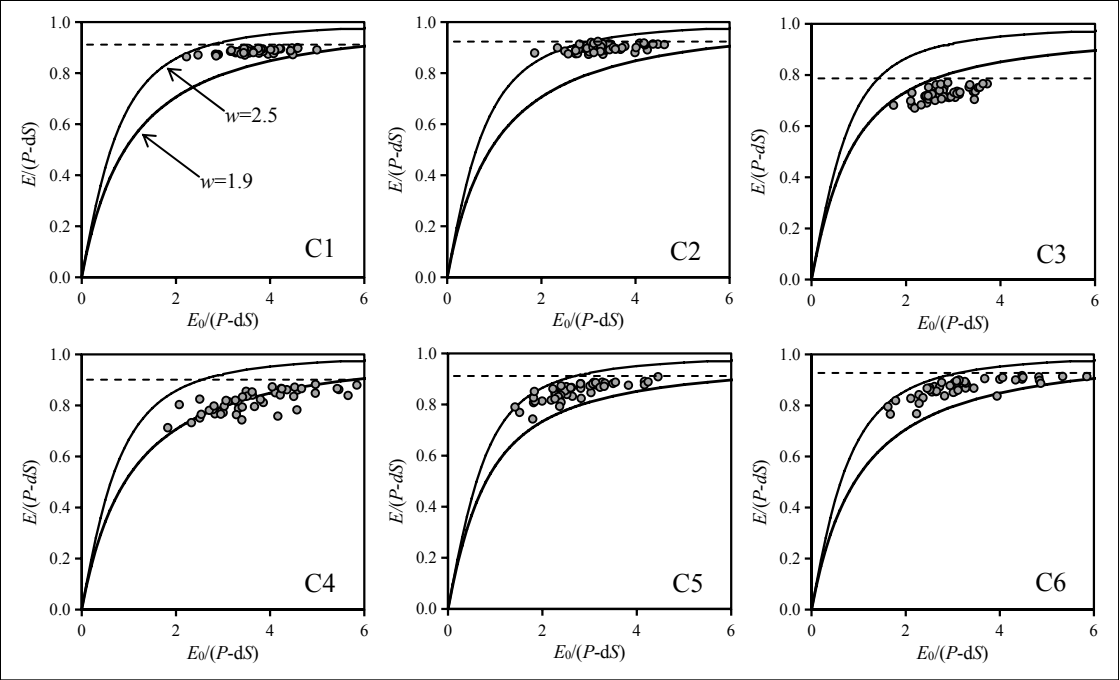
E/(P-dS)
E0/(P-dS)
w=2.5
w=1.9
C1
C2
C3
C4
C5
C6

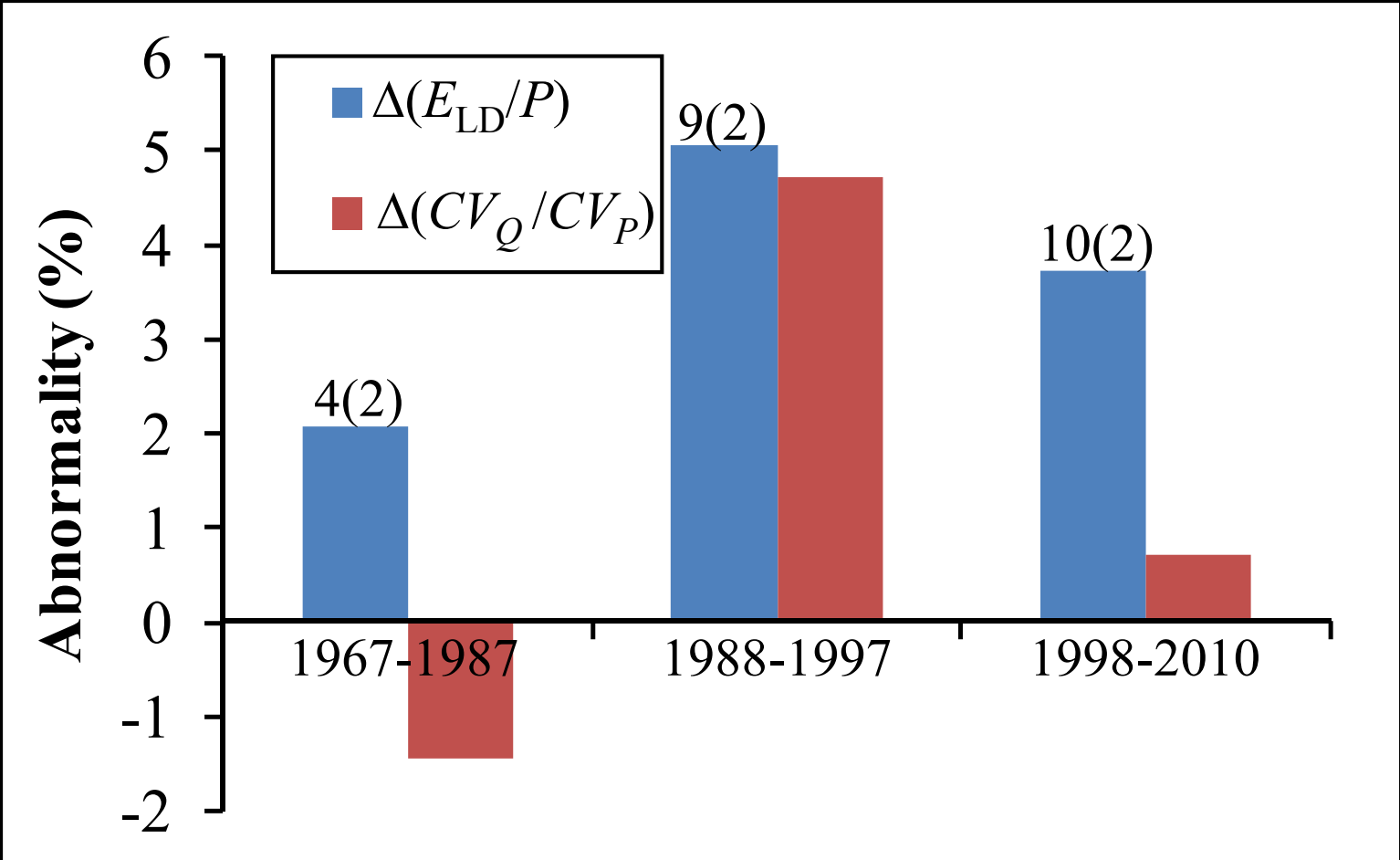
Abnormality (%)
6
5
4
3
2
1
0
-1
-2
$\Delta(E_{LD}/P)$
$\Delta(CV_Q/CV_P)$
4(2)
9(2)
10(2)
1967-1987
1988-1997
1998-2010